Advances in Energy Research, *Vol. 2, No. 1 (2014) 47-59*
DOI: http://dx.doi.org/10.12989/eri.2014.2.1.047

Transient stability improvement using quasi-multi pulse BTB-STATCOM

Ahmet M. Vural*[1a] and Kamil C. Bayindir[2b]

[1]Department of Electrical and Electronics Engineering, Gaziantep University, Gaziantep, Turkey
[2]Department of Electrical and Electronics Engineering, Cukurova University, Adana, Turkey

(Received November 11, 2013, Revised April 28, 2014, Accepted April 28, 2014)

Abstract. Back-to-back STATCOM configuration is an extension of STATCOM in which the reactive power at two-sides and the real power flow through the DC link can be controlled concurrently and independently. This flexible operation brings many advantages to the micro-grids, distributed generation based systems, and deregulated power systems. In this paper, the dynamic control characteristics of the back-to-back STATCOM is investigated by simulating the detailed converter-level model of the converters in PSCAD. Various case studies in a single-machine test system are studied to present that the real power control feature of the BtB-STATCOM, even with a simple controller design, can enhance the transient stability of the machine under different fault scenarios.

Keywords: back-to-back STATCOM; quasi multi-pulse voltage source converter; real power flow control; reactive power control; voltage control; transient stability

1. Introduction

Back-to-back operation of high power converters enable load transfer between two interconnected (asynchronous) grids, without having to disconnect and then reconnecting it to the other system using mechanical switches. Besides this function, the reactive power hence bus voltage magnitude at the distribution/transmission level can be controlled effectively at the two-sides of the converters.

Back-to-Back Static Synchronous Compensator (BtB-STATCOM) is an example of back-to-back operation of high power converters and a multi-converter FACTS device constructed by joining two separate STATCOMs at their DC link in a substation. (Vural and Bayindir 2011, Larsson *et al.* 2001, Reed *et al.* 2003). In literature, instead of “BtB-STATCOM” as the compensator name, “BtB DC link” or “Voltage Source Converter (VSC) based BtB high voltage DC (HVDC) transmission link” are the alternative definitions (Tyagi and Padiyar 2006), Parkhidehet and Bhattacharya 2009, Xinghao *et al.* 2009). The concept can also be described as

*Corresponing Author, Ph.D., E-mail: metevural@hotmail.com
[b] Ph.D., E-mail: kcagataybayindir@gmail.com

http://www.techno-press.org/?journal=eri&subpage=7 ISSN: 2287-6316 (Print), 2287-6324 (Online)

VSC based HVDC without long transmission network. As a practical application example, a ± 72 MVA BtB-STATCOM consisting of two ± 36 MVA STATCOMs have been installed for the first time in Eagle Pass substation and in Piedras Negras substation to enable bi-directional real power transfer between USA and Mexico as well as reactive power support for dynamic voltage control at two distinct buses (Larsson *et al.* 2001).

A non-linear control scheme for BtB-STATCOM is developed using an average modeling approach (Lee *et al.* 2011). The stability studies are conducted on Phillips-Heffron model of SMIB system which includes the average model of two BtB VSCs Banaei and Taheri (2009). A supplementary control for VSC based BtB link in damping sub-synchronous resonance of series capacitive compensated transmission system is studied using an average model of each VSC (Faried *et al.* 2009).

Dynamic modeling of BtB-STATCOM is approximated using average modeling approach where each output of VSC is modeled as controllable ideal voltage source Tyagi and Padiyar (2006, Xinghao *et al.* 2009, Lee *et al.* 2011), Parkhidehet and Bhattacharya (2009). On the other hand, converter-level models of BtB-STATCOM are more detailed. For instance, two elementary two-level six-pulse converters are used in BtB-STATCOM configuration (Ruihua *et al.* 2005, Jovcic *et al.* 2007, Liu *et al.* 2010). Converter structure is pretty simple that does not reflect realistic BtB-STATCOM operation completely. More detailed converter topologies are alternatively considered. For instance quasi multi-pulse converter topology consisting of sixteen six-pulse units are combined to build each VSC of BtB-STATCOM (Hagiwara *et al.* 2003). The BtB system consists of two sets of four three-phase neutral-point-clamped converter units each having twelve GTOs driven by PWM Hagiwara and Akagi (2005), (Hagiwara *et al.* 2008). 24-pulse three-level voltage source converters with fundamental frequency switching for HVDC system is proposed (Madhan *et al.* 2009).

According to literature review results, transient stability studies of BtB-STATCOM generally rely on average models included into Phillips-Heffron Single-Machine Infinite-Bus (SMIB) system or multi-machine systems, rather than using converter-level models.

2. BtB-STATCOM Principle

The key-stone of BtB-STATCOM is the VSC which has a fast response and can be interfaced with any energy storage units. The STATCOM configuration is basically shown in Fig. 1 (Singh *et al.* 2009). During low voltage conditions STATCOM shows its superiority as the magnitude of the supplied reactive current is independent of the system voltage. However in a conventional compensator (SVC), the capacitive current drops linearly as system voltage reduces when high capacitive current is highly required. AC output of the converter is proportional to the DC link voltage. By controlling STATCOM voltage, the reactive current injected from the converter to the system bus can be controlled as well. Phase angle between STATCOM voltage and bus voltage becomes zero if converter losses are neglected. (Padiyar 2007).

In back-to-back configuration, each single STATCOM is connected in parallel to the system bus via shunt coupling transformer as shown in Fig. 2. Common DC link provides bi-directional real power transfer between two AC grids (synchronous or asynchronous or even with different frequencies). In addition each STATCOM can provide independent reactive power support for dynamic voltage control. It is observed that there are few papers regarding BtB-STATCOM in literature. In this research, the capabilities of BtB-STATCOM is investigated for dynamic bus

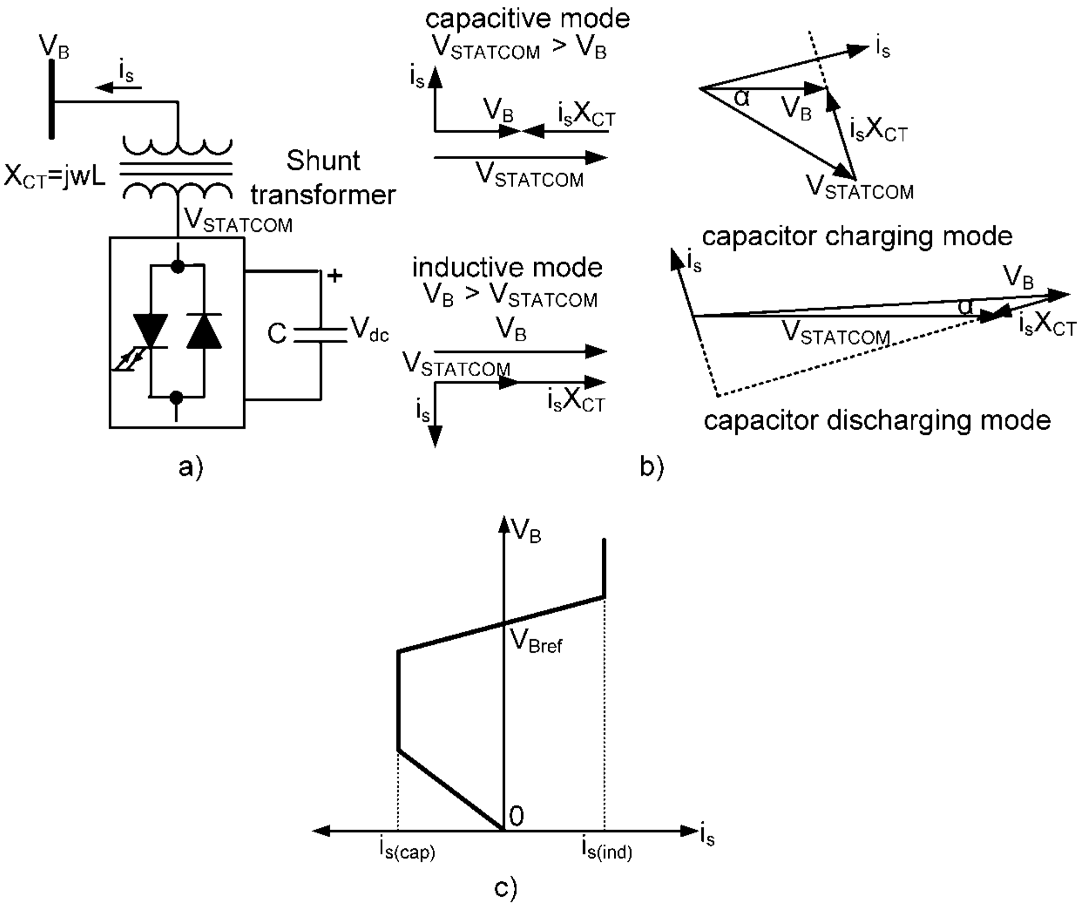

Fig. 1 STATCOM configuration (a) arrangement (b) operating modes

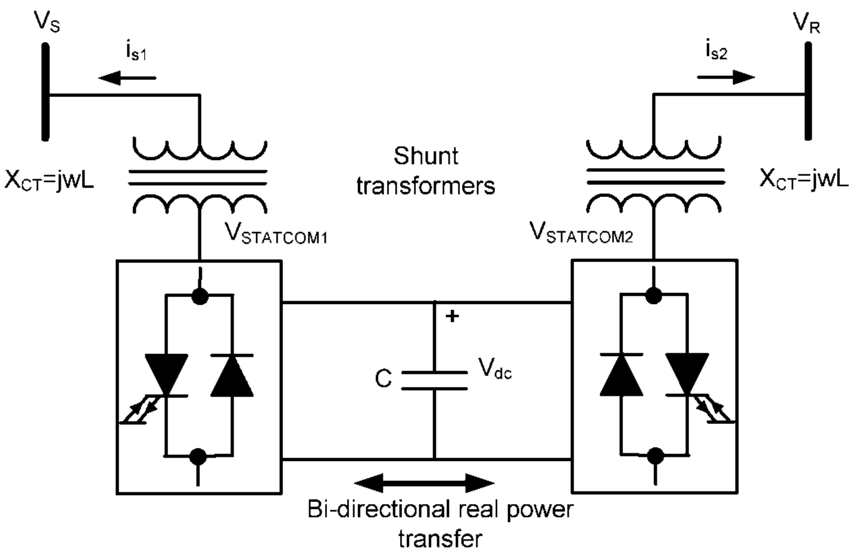

Fig. 2 BtB-STATCOM configuration with typical arrangement

voltage control, real power transfer capability, and damping out oscillations caused by severe disturbances.

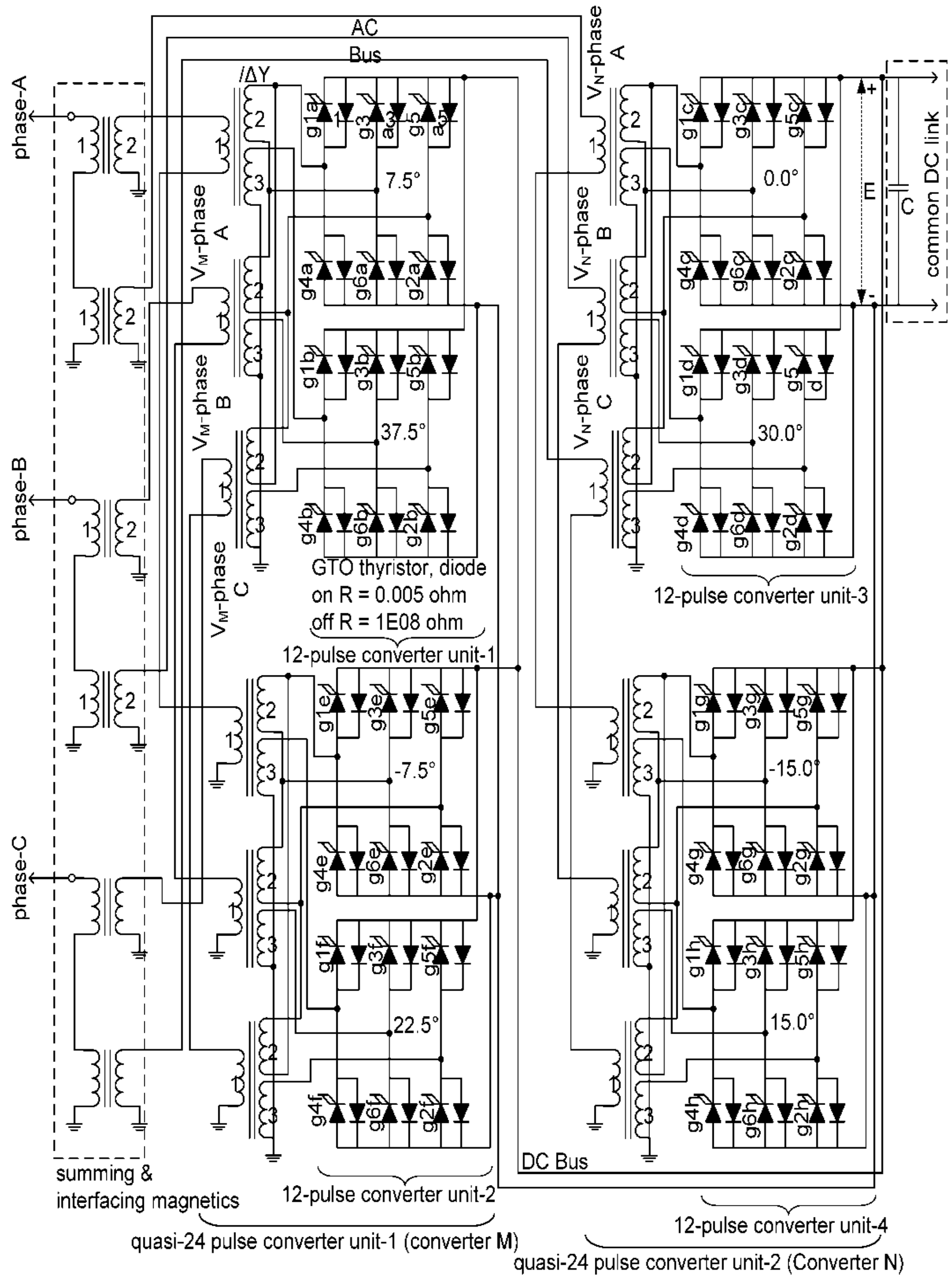

Fig. 3 Power circuit configuration of three-phase quasi multi-pulse VSC

3. Converter-level model of BtB-STATCOM

Converter-level model of BtB-STATCOM is realized using quasi multi-pulse converter topology as shown in Fig. 3 (Vural and Bayindir 2011). Each converter of BtB-STATCOM is comprised of the power circuit which consists of two identical converter groups (Converter M&N) as shown in Fig. 3. Each converter group is constructed from two twelve-pulse converter units to realize a quasi 24-pulse operation. Each phase of twelve pulse converter unit in either Converter M or N is coupled to the same phase of the second twelve-pulse converter unit using single-phase transformers. Each phase of Converter M is electromagnetically added to the same phase of Converter N using transformers. Summing and interfacing magnetics also couples VSC output voltage with the transmission level with no requirement to an extra shunt coupling transformer by adjusting the voltage ratings of the primaries of the transformers. There should be a 7.5° phase shift between two adjacent twelve-pulse converter units (Singh *et al.* 2009). At the same time, gating signals of each lower six-pulse converter in the twelve-pulse configuration should be shifted by 30° with respect to the upper six-pulse converter for twelve-pulse operation.

4. The study system

In order to investigate BtB-STATCOM behavior under large disturbances, the SMIB system shown in Fig. 4 is simulated for the study purpose when fault scenarios in different case studies are separately applied. Shunt converters VSC1 and VSC2 of the BtB-STATCOM are positioned at Buses 1 and 2, respectively by means of shunt coupling interfaces, tr1 and tr2. It is aimed to provide controlled real power transfer from 120 MVA rated SG to the infinite bus, while regulating neighboring bus voltages by means of BtB-STATCOM. The control schemes of the two converters are also depicted in Figure 6.21. SG is driven by hydro-governor with solid-state exciter. Simulated system has two 50 km transmission lines having data identical to the line positioned between Buses 1 and 4 in Section 6.4 with base values of 100 MVA, 154 kV, and 60 Hz. Test system and BtB-STATCOM having two quasi multi-pulse VSCs, and the control blocks are simulated in PSCAD with a solution time step of 100 μs. Each VSC of BtB-STATCOM is rated at 100 MVA. Each single-phase three-winding transformer in twelve-pulse converter unit is rated at 60 Hz, 8.33 MVA, 20/2/1.1548 kV with a leakage reactance of j0.1 pu. Each single-phase transformer of summing and magnetic interface is rated at 60 Hz, 16.67 MVA, 137.92/38 kV, j0.1 pu.

5. Simulation studies

The stability of the SMIB system is investigated without and with BtB-STATCOM having the PI control schemes shown in Fig. 4. By applying different types of faults with different durations the damping ability of the BtB-STATCOM is tested and evaluated for different cases. The impact of these faults is also investigated on the dynamic performances of the control loops. PI controller parameters of the BtB-STATCOM are given in Table 1. The capacitance of DC link is C=0.2 F. Using switches sw1 and sw2, BtB-STATCOM can be bypassed with a line, required for the

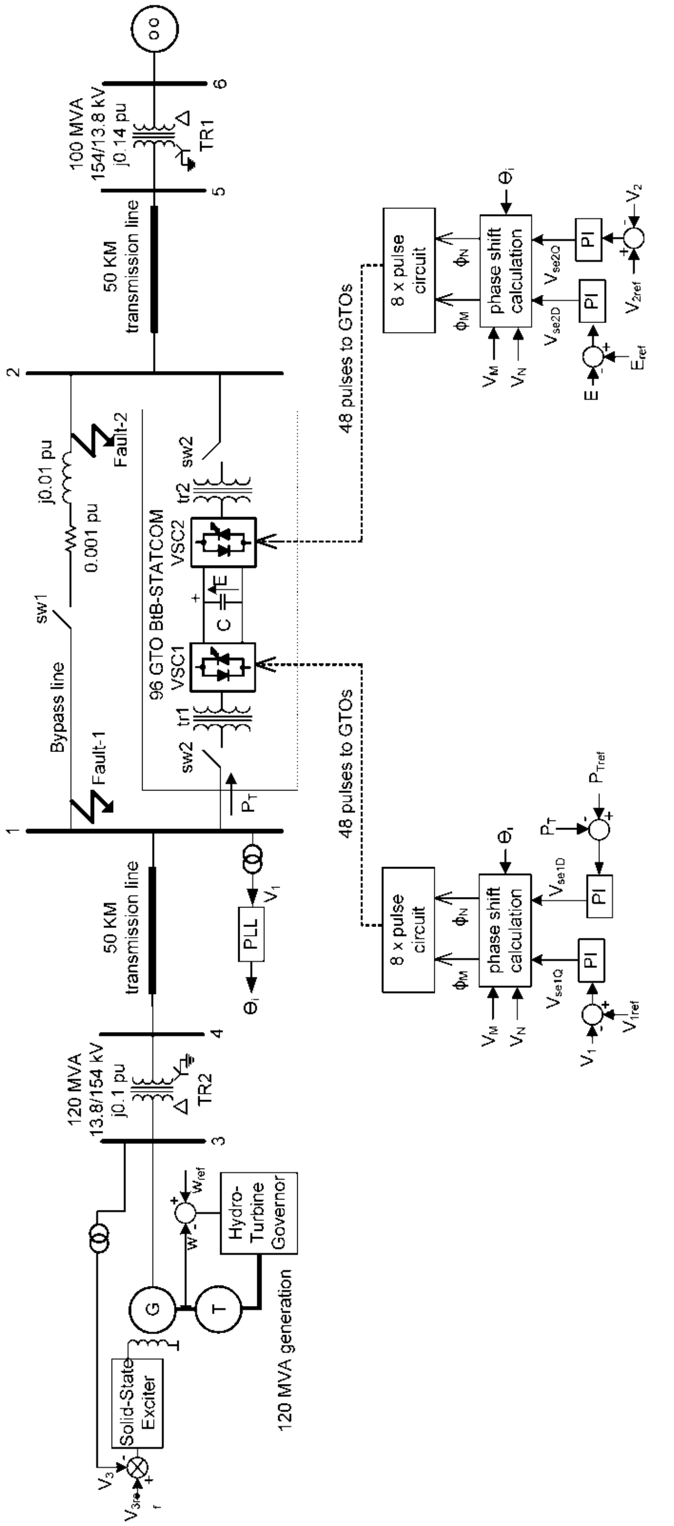

Fig. 4 Power system configuration embedded with BtB-STATCOM

Table 1 The PI controller parameters of the BtB-STATCOM

Proportional gain - Kp	Integral time constant - τ_i
VSC1, AC voltage controller = 0.8	VSC1, AC voltage controller = 0.01
VSC1, Real power transfer controller = 0.8	VSC1, Real power transfer controller = 0.01
VSC2, AC voltage controller = 0.8	VSC2, AC voltage controller = 0.01
VSC2, DC voltage controller = 0.1	VSC2, DC voltage controller = 0.1

simulation cases. For instance, when sw1 is closed while sw2 is opened, BtB-STATCOM is bypassed by a short line. When sw1 is opened while sw2 is closed, BtB-STATCOM is in operation alternatively. The following dynamic control tasks of the BtB-STATCOM are examined for different disturbance conditions:

Bus-1 voltage control by VSC1 of BtB-STATCOM
Bus-2 voltage control by VSC2 of BtB-STATCOM
DC link voltage by VSC2 of BtB-STATCOM
Real power transfer control by VSC1 of BtB-STATCOM

5.1 Case 1: three-phase to ground fault at generator bus

Three-phase to ground fault at 30.0 s for a duration of 120 ms is applied near Bus 1 in Fig. 4. Simulated waveforms of the SMIB system embedded with BtB-STATCOM following this severe disturbance are presented in Fig. 5. Fig. 5(a) shows that SG speed under the fault decreasingly oscillates for about 15 s when BtB-STATCOM is deactivated, but returns to its steady-state value with a slight drop when BtB-STATCOM is in operation. The 0.0015 pu steady-state speed difference is due to different demanded real power from SG in two different cases. The nominal value of the real power exchange from Bus 1 to Bus 2 is around 0.45 pu (45 MW) when a short line connects these two buses. Following fault, real power exchange oscillates for a duration of around 8 s as shown in Fig. 5(b). With the inclusion of BtB-STATCOM which ties neighboring buses, the oscillation is almost damped out with a steady-state increase of real power exchange to 0.8 pu (80 MW). Fig. 5(c) shows that the DC link voltage of the BtB-STATCOM decreases for a short time when the fault occurs at Bus 1 and restored to its controlled value immediately, not affecting the operation of BtB-STATCOM. Reactive power demand of SG in Fig. 5(d) is temporarily increased under the fault, but it restores immediately without losing stability when the fault is cleared. Fig. 5(e) and 5f depicts that the dynamic voltage support within the study system is effectively provided by BtB-STATCOM at two neighboring buses under the three-phase fault. Fig. 6 shows the traces of simulated voltage and current waveforms of BtB-STATCOM converters following three-phase fault. Fig. 7 shows the traces of simulated phase shift angles (ϕM and ϕN) and selected GTO's anode-to-cathode voltages of BtB-STATCOM converters following three-phase fault.

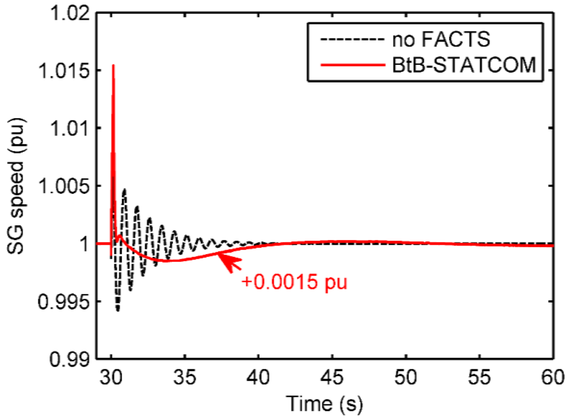

(a) Transient response of SG speed following three-phase fault

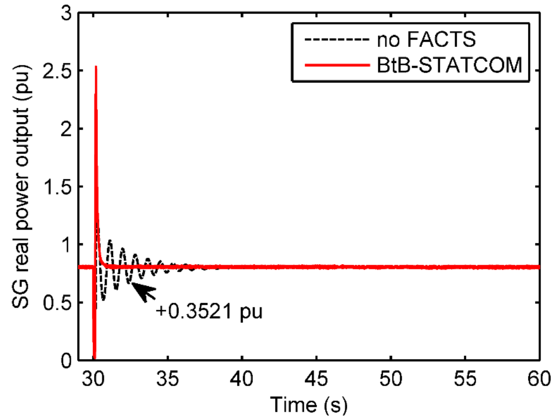

(b) Transient response of SG real power output following three-phase fault

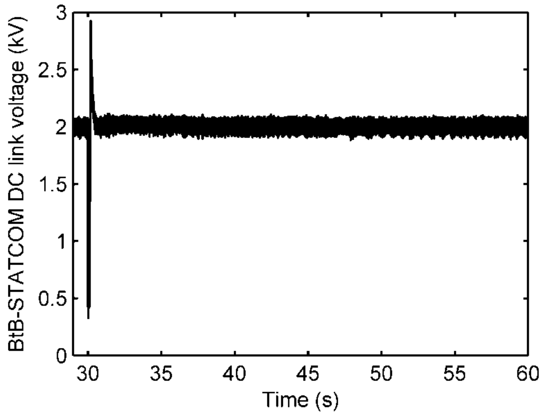

(c) DC link voltage excursions of BtB-STATCOM following three-phase fault

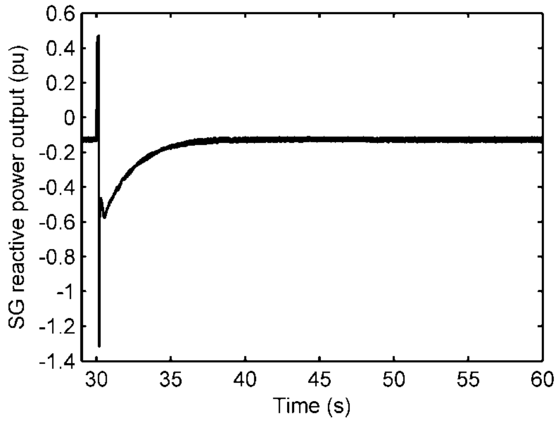

(d) Variation of SG reactive power output following three-phase fault

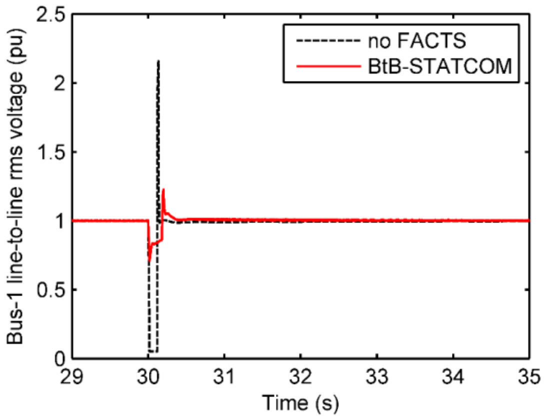

(e) Variation of Bus 1 voltage following three-phase fault

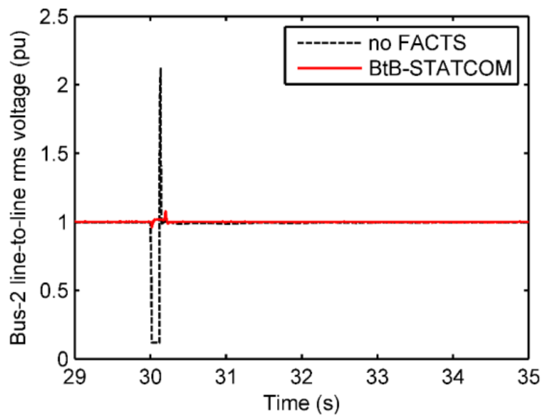

(f) Variation of Bus 2 voltage following three-phase fault

Fig. 5 Simulated BtB-STATCOM performance in case 1

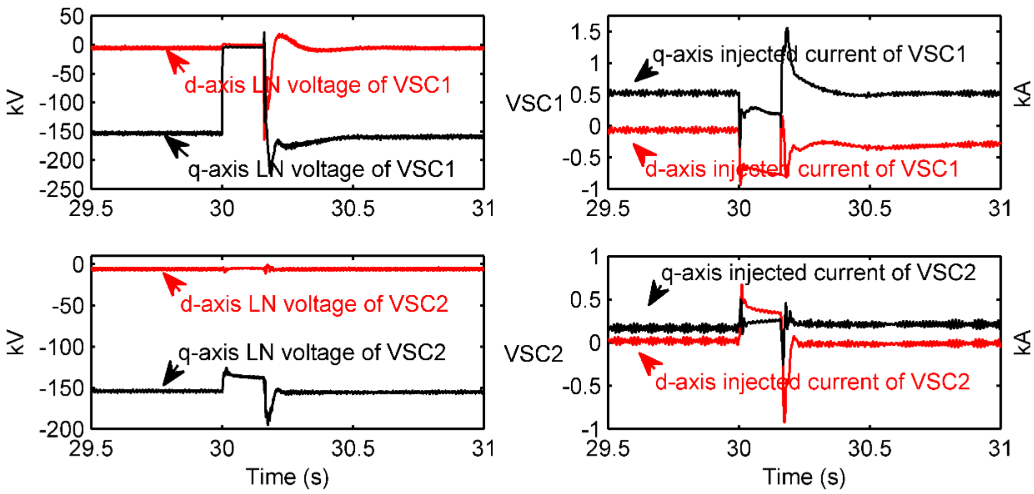

Fig. 6 Simulated voltage and current waveforms of the converters

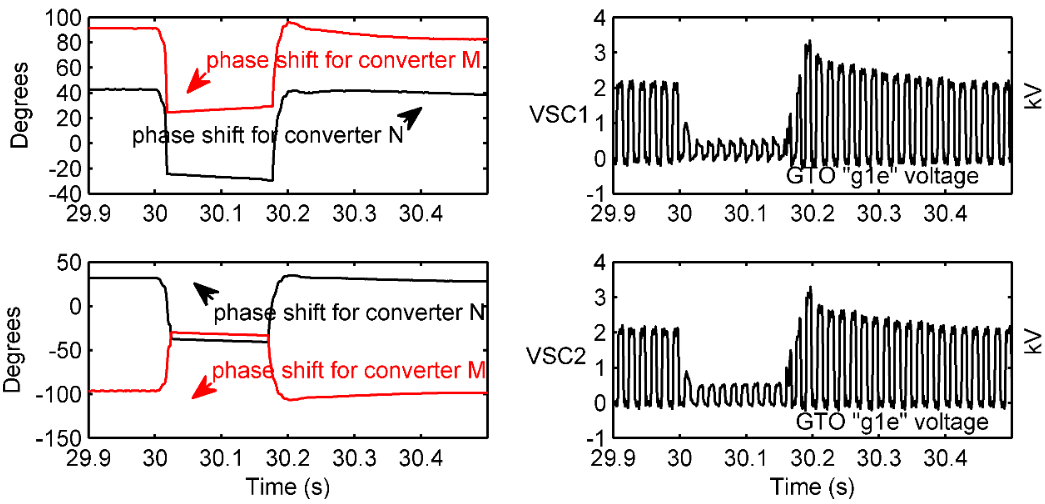

Fig. 7 Simulated phase shift angles (ϕ_M and ϕ_N) and one GTO voltage

5.2 Case 2: three-phase to ground fault at infinite bus

In this case, a relatively longer three-phase to ground fault is applied near Bus 2 (infinite bus) in Fig. 4. The fault is lasted for 160 ms. Simulated waveforms of the power system configuration embedded with BtB-STATCOM following the disturbance are presented in Fig. 8. The speed oscillations of the SG like the one in previous case study are observed in Fig. 8(a) when BtB-STATCOM is deactivated. The oscillation duration is relatively shorter than that of previous case since there is short line between SG and the fault location. When BtB-STATCOM is activated, SG speed oscillation is better damped out when compared with the previous case study. Moreover the slight drop in speed is not observed following three-phase fault. This is due to the fact that the fault is occurred near a stiff bus and BtB-STATCOM isolates the disturbance from

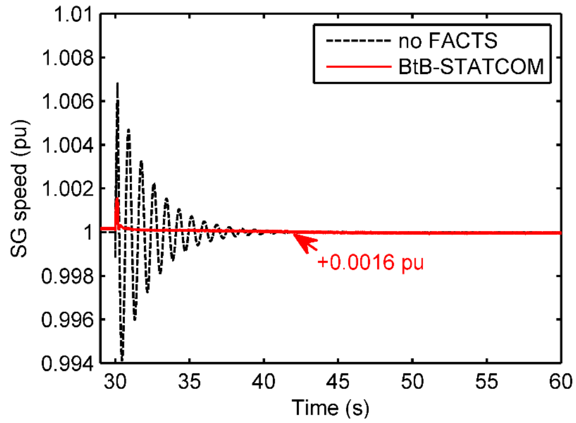

(a) Transient response of SG speed following three-phase fault

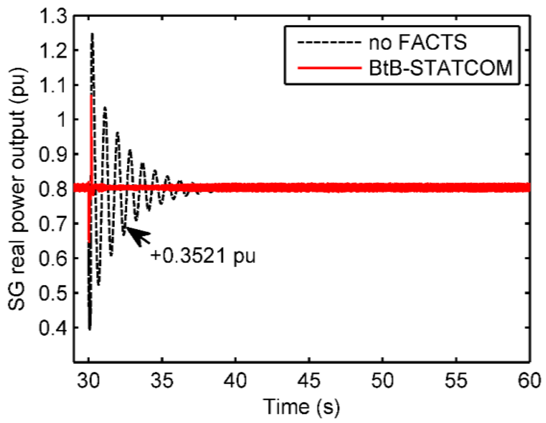

(b) Transient response of SG real power output following three-phase fault

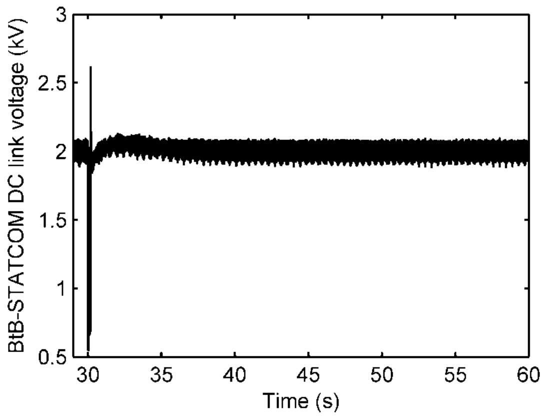

(c) DC link voltage excursions of BtB-STATCOM following three-phase fault

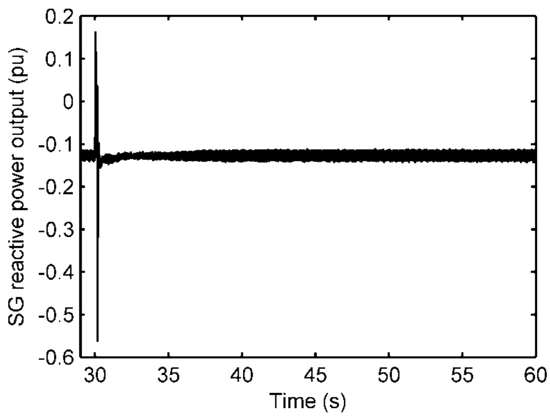

(d) Variation of SG reactive power output following three-phase fault

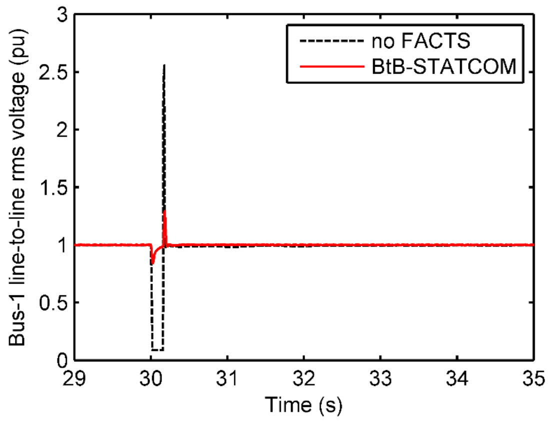

(e) Variation of Bus 1 voltage following three-phase fault

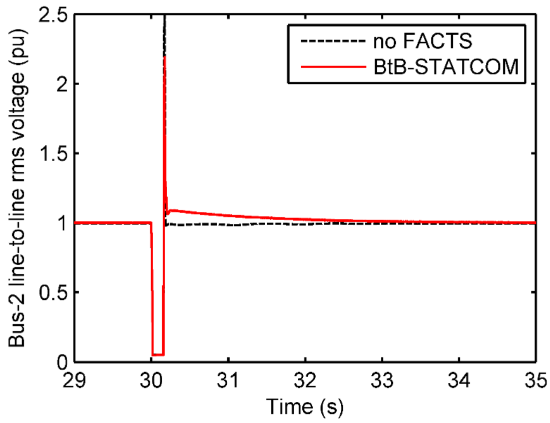

(f) Variation of Bus 2 voltage following three-phase fault

Fig. 8 Simulated BtB-STATCOM performance in case 2

Table 2 THD values of power system bus voltages

Case 1	THD $V_{1(\text{L-L})}$	THD $V_{2(\text{L-L})}$	Case 2	THD $V_{1(\text{L-L})}$	THD $V_{2(\text{L-L})}$
	1.38 %	1.36 %		1.37%	1.36%

SG with its converters. The same steady-state speed difference of the SG (0.0015 pu) is observed like the one in previous case study, due to the same loading condition of the SG as expected. In Fig. 8(b), the maximum overshoot of the controlled SG real power output (0.8 pu) is significantly reduced in this case with a better response of the BtB-STATCOM to the fault. The DC link voltage fall in Fig. 8(c) is unavoidable. However, as soon as the fault is cleared, DC link voltage restores to its reference without affecting BtB-STATCOM operation. Reactive power demand of the SG in Fig. 8(d) restores immediately to its pre-fault value as soon as the fault is cleared. A less undershoot shows up than that of previous case due to the fault isolation feature of the BtB-STATCOM. Figs. 8(e) and (f) depicts that the dynamic voltage support within the study system is effectively provided by BtB-STATCOM at two neighboring buses under the three-phase fault. In detail, the drop in Bus 2 voltage is not avoided. However the voltage is controlled with less overshoot when BtB-STATCOM is activated.

5.3 THD Content

Voltage distortions at Buses 1 and 2 as a measure of THD are listed in Table 6.5. Records of the simulated cases show that THD values are within acceptable limits when BtB-STATCOM is in operation IEEE (1993). Even GTOs are switched at fundamental system frequency, filtering is not required due to low THD content.

6. Discussion

It is shown that BtB-STATCOM, although not utilized primarily for enhancing power system stability, can also be used to damp out generator speed oscillations effectively even with simple PI controllers without any speed signal measurement. DC power transmission among the two VSCs enables both controlled real power exchange from one bus to another and improving power system stability with the feature of isolating the fault from the rest of the power system. As it can be seen the oscillations in the DC link are hardly noticeable. The internal simulated signals of BtB-STATCOM show that the stable operation can be achieved both in steady- and transient states in case of a severe disturbance while providing reactive power to the neighboring buses for voltage control. Near-full rate of the converters with low THD content are achieved by setting the reference value of the real power exchange among the two VSCs to relatively a large value of 0.8 pu.

7. Conclusions

Multi-control function of the BtB-STATCOM is examined without any damping control scheme for improving power system stability considering various faults with different locations and durations. The obtained results confirm that the real power transfer controller of PI type of BtB-STATCOM can provide adequate damping of generator speed oscillations owing to the segmentation of the power system with the DC link of BtB-STATCOM. At the same time, it is ensured that all BtB-STATCOM control loops are working truly without losing stability under different fault scenarios. Voltage profiles of the neighboring buses are also improved with fast and independent reactive power support of BtB-STATCOM converters in both steady- and transient states. This study reveals the potential usage and benefits of BtB-STATCOM applications for intelligent control of future grids having distributed energy resources, with emphasis on high power applications of converters with a low THD content.

References

Banaei, M.R. and Taheri, N. (2009), "HVDC based damping controllers for power system stability, *31st International Telecommunications Energy Conference*, Incheon, October.

Faried, S.O., Tang, G. and Edris, A. (2009), "Supplemental control of voltage sourced converter-based back-to-back for damping subsynchronous resonance", *IEEE Power & Energy Society General Meeting*, Calgary, July.

Hagiwara, M. and Akagi, H. (2005), "An approach to regulating the DC-link voltage of a voltage-source BTB system during power line faults", *IEEE Transactions on Industry Applications*, **41**(5), 1263- 1271.

Hagiwara, M., Fujita, H. and Akagi, H. (2003), "Performance of a self-commutated BTB HVDC link system under a single-line-to-ground fault condition", *IEEE Transactions on Power Electronics*, **18**(1), 278-285.

Hagiwara, M., Phuong, V.P. and Akagi, H. (2008), "Calculation of DC magnetic flux deviation in the converter-transformer of a self-commutated BTB system during single-line-to-ground faults", *IEEE Transactions on Power Electronics*, **23**(2), 698-706.

IEEE (1993), "IEEE recommended practices and requirements for harmonic control in electrical power systems", *Institute of Electrical and Electronics Engineering*, April 1993.

Jovcic, D., Lamont, L. and Abbott, K. (2007), "Control system design for VSC transmission", *Electr. Pow. Syst. Res.*, **77**(7), 721-729.

Larsson, T., Petersson, A., Edris, A., Kidd, D. and Aboytes, F. (2001), "Eagle pass back-to-back tie: a dual purpose application of voltage source converter technology", *IEEE Power Engineering Society Summer Meeting*, Vancouver, July.

Lee, Y.O, Kang, H.J., Han, Y. and Chung, C.C. (2011), "A nonlinear control for a BTB STATCOM system with asymmetrically structured converters", *IEEE Trondheim PowerTech*, Trondheim, June.

Liu, J. Tang, Y., Sun, H., Xue, M. and Liu, B. (2010), "Control strategy for power grids synchronism parallel based on back-to-back VSC", *International Conference on Power System Technology*, Hangzhou, October.

Madhan, M. D., Singh, B. and Panigrahi, B.K. (2009), "Harmonic optimised 24-pulse voltage source converter for high voltage DC systems, *IET Power Electronics*, **2**(5), 563-573.

Padiyar, K.R. (2007), *FACTS Controllers In Power Transmission And Distribution*, New Age International Publishers, New Delphi, India.

Parkhideh, B. and Bhattacharya, S. (2009), "Resilient operation of voltage-sourced BTB HVDC systems under power system disturbances", *IEEE Power & Energy Society General Meeting*, Calgary, July.

Reed, G., Pape, R. and Takeda, M. (2003), "Advantages of voltage sourced converter (VSC) based design concepts for FACTS and HVDC-link applications", *IEEE Power Engineering Society General Meeting*, Calgary, July.

Ruihua, S., Chao, Z., Ruomei, L. and Xiaoxin, Z. (2005), "VSCs based HVDC and its control strategy", IEEE/PES Transmission and Distribution Conference and Exhibition: Asia and Pacific, Dalian.

Singh, B., Saha, R., Chandra, A. and Al-haddad, K. (2009), "Static synchronous compensators (STATCOM):

a review", *IET Power Electronics*, **2**(4), 297-324.
Tyagi, A. and Padiyar, K.R. (2006), "Dynamic analysis and simulation of a VSC based back-to-back HVDC link", *India International Conference on Power Electronics*, Chennai, December.
Vural, A.M. and Bayindir, K.C. (2011), "Quasi multi-pulse back-to-Back static synchronous compensator employing line frequency switching 2-level GTO inverters", *World Academy of Science, Engineering and Technology*, **60**, 1863-1874.
Xinghao, F. and Chow, J.H. (2009), "BTB DC link modeling, control, and application in the segmentation of AC interconnections", *IEEE Power & Energy Society General Meeting*, Calgary, July.

CC